Published in final edited form as:
Development. 2005 January ; 132(1): 155–164.

Drosophila retained/dead ringer is necessary for neuronal pathfinding, female receptivity and repression of *fruitless* independent male courtship behaviors

Lynn M. Ditch[1,2,3], **Troy Shirangi**[1], **Jeffrey L. Pitman**[1,2], **Kristin L. Latham**[4], **Kim D. Finley**[2,*], **Philip T. Edeen**[2,†], **Barbara J. Taylor**[4], and **Michael McKeown**[1,2,‡]

1*Molecular Biology, Cell Biology, and Biochemistry Department, Brown University, Providence, RI 02912, USA*

2*Molecular Biology and Virology Laboratory, The Salk Institute for Biological Studies, La Jolla, CA 92037, USA*

3*Department of Biology, University of California, San Diego, La Jolla, CA 92093, USA*

4*Department of Zoology, Oregon State University, Corvallis, OR 97331, USA*

Summary

Mutations in the *Drosophila retained/dead ringer* (*retn*) gene lead to female behavioral defects and alter a limited set of neurons in the CNS. *retn* is implicated as a major repressor of male courtship behavior in the absence of the *fruitless* (*fru*) male protein. *retn* females show *fru*-independent male-like courtship of males and females, and are highly resistant to courtship by males. Males mutant for *retn* court with normal parameters, although feminization of *retn* cells in males induces bisexuality. Alternatively spliced RNAs appear in the larval and pupal CNS, but none shows sex specificity. Post-embryonically, *retn* RNAs are expressed in a limited set of neurons in the CNS and eyes. Neural defects of *retn* mutant cells include mushroom body β-lobe fusion and pathfinding errors by photoreceptor and subesophageal neurons. We posit that some of these *retn*-expressing cells function to repress a male behavioral pathway activated by fru^{M}.

Keywords

Courtship; Behavior; *retained*; *fruitless*; Neuronal pathfinding; *Drosophila*

Introduction

Courtship in *Drosophila* provides a genetic, molecular, and neurological model for behavioral development. During courtship, males and females perform gender-specific behaviors (reviewed by Greenspan and Ferveur, 2000). The male begins by following the female, tapping her abdomen, and extending and vibrating one wing to produce a species-specific ‘love song’. A virgin female initially runs from the male, but if receptive, she slows and positions herself to facilitate copulation.

This binary behavioral system is controlled by the sex differentiation cascade (Hall, 1994;Yamamoto et al., 1998;O’Kane and Asztalos, 1999;Goodwin, 1999;Christiansen et al.,

‡Author for correspondence (e-mail: michael_mckeown@brown.edu)
*Present address, Cellular Neurobiology Laboratory, The Salk Institute, PO Box 85800, San Diego, CA 92186-5800, USA
‡Present address, Ambit Biosciences, San Diego, 4215 Sorrento Valley Boulevard, San Diego, CA 92121, USA

2002). *Sex-lethal* (*Sxl*), *transformer* (*tra*) and *transformer 2* (*tra2*) catalyze splicing of the next step of the pathway, leading to the activation of sex-specific forms of *doublesex* (*dsx*) and *fruitless* (*fru*). *dsx* controls external differentiation, yolk protein synthesis, aspects of male song production (Villella and Hall, 1996) and potentially some aspects of female neural differentiation (Waterbury et al., 1999). *fru* determines many aspects of male courtship and copulatory behaviors, but has no apparent role in female sexual development (Ryner et al., 1996;Ito et al., 1996;Gailey et al., 1991;Villella et al., 1997). *dissatisfaction* (*dsf*) females resist males during courtship, whereas *dsf* males are bisexual (Finley et al., 1997;Finley et al., 1998). Many male courtship mutants have been identified, while few mutations linked to female receptivity have been characterized (Yamamoto et al., 1997).

We identified *retained/dead ringer* (*retn*) from a genetic screen for female behavioral mutations. *retn* females are resistant to courtship, and show *fru*-independent male-like courtship behaviors, while *retn* males are behaviorally normal. These sex-specific effects on behavior do not correlate with sexually distinct expression or splicing patterns in the CNS. Examination of *retn* cells in *retn* mutant backgrounds reveals aberrant projections by mushroom body, photoreceptor and subesophageal neurons. *retn* affects development of sex-specific neurons, and may repress male behavior patterns in the female CNS.

Materials and methods

Fly strains and behavioral assays

Fly stocks for the EMS screen are from Charles Zuker. UAS-*retn* and balanced *retn*-Gal4^{89}, *retn*-Gal4^{28}, *retn*-Gal4^{108}, *retn*-Gal4^{117}, *retn*-Gal4^{139}, *dri*^{1}, *dri*^{2}, *dri*^{3}, *dri*^{5}, *dri*^{6}, *dri*^{8}, *dri*^{B142} stocks were donated by Tetyana Shandala. *retn*^{RU50}, *retn*^{RO44} lines are from Trudi Schupbach. UAS-*tra* is from Ralph Greenspan. Additional lines were provided by the Bloomington Stock Center, Illinois. Control is Canton-S. Flies were raised on standard media.

Female resistance and male courtship indices were tested as previously described (Finley et al., 1997). Male-male courtship and female bisexuality were tested in groups of 10 animals and quantitated as number of courtship events per 5-minute interval. A courtship event was counted as one fly following, tapping or singing to a target fly for a minimum of 2 seconds. Multiple trials were carried out for each genotype and age. All P-values are derived from two-tailed paired *t*-tests. Multiple *retn*-Gal4 lines were used to drive UAS-*retn*, UAS-*Tra*^{F} and UAS-*GFP*. All generated the same pattern and had similar effects. *retn*-Gal4^{89}, a lethal insertion, showed the most complete rescue of female resistance behavior and egg laying, and was primarily used for studies of *retn* function and expression. Rescue of male-like behaviors in females was complicated by inconsistency of these behaviors in *retn*-Gal4/*retn* mutants.

Sequencing

Genomic DNA from *retn*$^{z2\text{-}428}$, *retn*^{RO44}, *retn*^{RU50}, *retn*^{dri1} and *retn*^{driB142} flies was amplified by PCR. Purified PCR product was sequenced at the Salk Sequencing Facility (La Jolla, CA). Sequences were assembled using DNA Sequencher (Gene Codes Corp, Ann Arbor, MI). Sequence comparison and database searches utilized BLAST (Altschul et al., 1990) and/or FASTA (Pearson and Lipman, 1988).

RETN fusion and mutant expression: EMSA

Full-length *retn* cDNA was generated by PCR, using genomic DNA from UAS-*retn* flies. The cDNA product was cloned into pBluescript-SK+ (pBS, Stratagene) and sequenced on both strands.

To produce ARID-box subclones, the pBS-*retn* plasmid was used as template for further PCR. The subsequent $retn_{ARID}$ product encodes amino acids 230-500 of RETN, and includes the ARID domain plus flanking sequence. This was subcloned into pBS and sequenced on both strands. pGEX-$retn_{ARID}$ was produced by inserting a *Bam*HI-*Xho*I fragment of pBS-$retn_{ARID}$ into the *Bam*HI and *Sal*I sites of pGEX-KG.

BS-$retn^{RO44}{}_{ARID}$ and BS-$retn^{z2\text{-}428}{}_{ARID}$ vectors were generated using PCR-based site-directed mutagenesis of the pBS-$retn_{ARID}$ template. Positive clones were confirmed by sequencing and transferred into pGEX-KG.

DNA-binding analysis was performed as described by Pitman et al. (Pitman et al., 2002). RETN wild-type and mutant fragments were expressed as GST-RETN fusion proteins in BL21 *pLysS* bacteria. Proteins were purified and eluted (Kaelin et al., 1992). EMSA analysis used 2μl of eluted protein. Proteins were tested for relative expression on a western blot, using rabbit anti-GST antibodies.

RT-PCR

For examination of *retn* RNA, CNS tissue (sans imaginal discs) was isolated from both sexes of late third instar larvae or mid-stage pupae. Total RNA was extracted using RNeasy Mini Kit (Qiagen). An antisense primer targeted to either exon 11 or 12 of *retn* was used to prime DNA synthesis by M-MLV Reverse Transcriptase (Sigma). A first round of PCR was carried out using primers against exons 1 and 4, 4 and 8, 8 and 11, 8 and 12, 1 and 8, and 4 and 11. A second round of PCR was then carried out using primers internal to those used in the first round. For examination of *fru* P1-derived RNAs in *retn* mutants, RNA was isolated from mid-pupal CNS tissue and from adult heads. For analysis of *fru* P1 RNAs in *retn fru* double mutants, RNA was isolated from adult heads. The RT-PCR procedure was as above with *fru* primers. For all *fru* RNA tests, reverse transcription was primed from within exon 3, which is common to all *fru* RNAs. The 3′ primer for both first and second round PCR was placed just inside (more 5′ on the RNA) to the RT primer. For analysis of the *fru*M RNA, first round PCR was primed at the 5′ side from within promoter P1-derived exon 2. Second round PCR used a primer just 3′ of this. For analysis of the *fru*F RNA, first and second round 5′ primers were just upstream of the TRA/TRA2 activated splice site of *fru*.

Microscopy

Confocal images were obtained on Zeiss LSM 480 and LSM510 Meta microscopes, using Renaissance 410 (Microcosm, Columbia, MD) software. Antibodies to Fas2 were obtained from the Developmental Studies Hybridoma Bank (University of Iowa). The brains of mutant and wild-type males and females were labeled with anti-Fasciclin 2 (Fas2) (1:20) and then with an anti-mouse secondary Alexa 488 (1:200; Molecular Probes) using standard methods (Finley et al., 1997).

Results

Identification and mapping of *retn*

We conducted a genetic screen similar to the screen that identified *dsf* (Finley et al., 1997), testing a collection of viable EMS-treated chromosomes developed in C. Zuker's laboratory. One of these lines, *z2-428*, showed substantial alterations in female behavior and fertility. Recombination and deficiency mapping place *z2-428* in salivary chromosome region 59F, between the right-hand breakpoint of Df(2R)bw5 and the left-hand breakpoint of Df(2R) HB132. These deletions complement *z2-428*. Additional testing revealed that *z2-428* is allelic to *retn*, an uncloned female sterile locus (Schupbach and Wieschaus, 1991).

Alleles of *dead ringer* (*dri*), an extended ARID (AT-rich interaction domain) Box-Family embryonic DNA-binding factor (Gregory et al., 1996;Iwahara et al., 2002) also fail to complement *retn*. We sequenced the exons and exon/intron boundaries of *dri* in *z2-428*, $retn^{RO44}$ and $retn^{RU50}$ (Fig. 1). Each allele has a single nucleotide change in the *dri*-coding region, corresponding to an ARID box amino acid substitution. Two *dri* lethal alleles, dri^{1} and dri^{B142}, encode premature stop codons, truncating the protein (Fig. 1). Thus, missense alleles $retn^{z2\text{-}428}$, $retn^{RU50}$ and $retn^{RO44}$ encode a protein with sufficient function that mutant progeny survive to adulthood, while nonsense alleles are lethal.

Drosophila convention favors earlier over later names of the same locus. Thus, FlyBase now refers to *retn* and *dri* as *retn*. We distinguish *retn*-class alleles, which are adult viable with behavioral and reproductive defects, from *dri*-class alleles, which are embryonic lethal. We denote dri^{1}, *dri*-$Gal4^{89}$ and other lethal alleles as $retn^{dri1}$, *retn*-$Gal4^{89}$, etc.

ARID box point mutants affect viability

retn mutant proteins have residual DNA-binding ability (data not shown) consistent with survival of some mutant individuals to adult stages. We asked whether these mutations alter the vital function of *retn* and to what extent phenotypes may be limited to later functions. In examining viability of *retn* heteroallelic combinations, we found variability in eclosion rates (Fig. 2A) with most lethality in the larval stages. Allelic strength in terms of pre-adult mortality is $retn^{dri2}$ > $retn^{dri1}$ > *retn*-$Gal4^{89}$ > $retn^{dri8}$ > $retn^{z2\text{-}428}$ > $retn^{RU50}$ > wild-type. $retn^{z2\text{-}428}$/$retn^{dri2}$ flies eclose with only 8% of expected rates, while $retn^{z2\text{-}428}$/$retn^{dri1}$ flies eclose with 25% of expected rates. $retn^{RU50}$/$retn^{dri1}$ and $retn^{RU50}$/$retn^{dri2}$ eclose with 65% and 68%, respectively, of expected numbers. P-element insertion alleles show full or nearly full viability with *retn*-class alleles. *retn* lethal alleles show no dominant lethality. Thus, all *retn*-class alleles at least partially complement the vital functions of *retn*. In addition, the *retn* cDNA rescues the partial lethality of $retn^{z2\text{-}428}$/*retn*-$Gal4^{89}$ (Fig. 2B). $retn^{z2\text{-}428}$/*retn*-$Gal4^{89}$ flies eclose with 33% of expected numbers, while $retn^{z2\text{-}428}$/*retn*-$Gal4^{89}$; UAS-*retn* flies eclose with 100% of expected numbers.

retn female receptivity

retn females are strikingly resistant to male courtship (Fig. 3A). Wild-type females, as well as *retn*/+, copulate after an average of three minutes or less of courtship. $retn^{RU50}$ and $retn^{z2\text{-}428}$ females showed significant increase in time of courtship prior to copulation: $retn^{RU50}$/$retn^{dri2}$ females average 34±6 minutes (P=0.00004), and $retn^{z2\text{-}428}$/$retn^{dri2}$ females typically resisted male advances for the entire hour in which we monitored courtship, averaging 58±2 minutes ($P=5\times10^{-17}$). $retn^{RU50}$/$retn^{z2\text{-}428}$ females showed a less severe phenotype, with an average of 8.8±2 minutes (P=0.013). Females showed virgin resistance behaviors of running, kicking, wing flicking and bending the abdomen away from males. Following copulation, females showed normal mated responses of ovipositor extrusion.

retn cDNA rescues female resistance

A *retn*-Gal4 enhancer trap (Brand and Perrimon, 1993) that is known to match the RETN protein pattern (Shandala et al., 1999) (J. Sibbons, personal communication) driving a UAS-controlled long form *retn* cDNA (Shandala et al., 1999) (see below) rescues female resistance behavior (Fig. 3B). *retn*-$Gal4^{89}$/$retn^{RU50}$; +/+ females resist courtship for an average of 25 ±4.6 minutes. *retn*-$Gal4^{89}$/$retn^{RU50}$; UAS-*retn*/+ females copulate in 4.8±1 minutes, comparable with wild type, and are fertile (L. M. Ditch, PhD thesis, University of California, 2002). This indicates that *retn*-Gal4 activates expression of UAS-*retn* in cells necessary for female behavior in a positionally and temporally correct pattern, and that overexpression of a non-sex-specific embryo-derived cDNA is sufficient to carry out some female neuronal functions.

retn females show male courtship behaviors

retn females show one behavior not shown by *dsf*, *dsx* or *fru* females: male-like courtship of females and males, especially as they age (Fig. 3C-F). *retn* females follow, tap and appear to sing. Although not as robust as male courtship – following is not as sustained, full wing extension and vibration are not seen, and copulatory bending is weak or absent – these behaviors highly resemble courtship.Fig. 3 shows still frames of this behavior, directed towards females (Fig. 3C,D) or a courting male (Fig. 3E). These behaviors vary between and within allelic combinations, but when the behaviors are seen they are striking and continue for hours. $retn^{z2\text{-}428}/retn^{dri8}$ females, which show the most consistent behaviors, with maximum penetrance at 3-4 weeks post-eclosion, averaged 42 courtship events per 5-minute observation period (Fig. 3F), while control females display fewer than three courtship-like events in the same period. Although male behaviors are evident, the *fru*M-dependent Muscles of Lawrence are not seen in *retn* females (not shown and L. M. Ditch, PhD thesis, University of California, 2002).

Aspects of the *retn* female behaviors are similar to wild-type female defenses of food and egg-laying resources. One study on *Drosophila* aggressive behaviors (Ueda and Kidokoro, 2002) indicated that aggression in wild-type females increases if females are raised individually before pairing for observation. We found no increase in male-like behaviors in females kept separately from eclosion until testing (not shown; L. M. Ditch, PhD thesis, University of California, 2002). This suggests that these behaviors are not an exaggerated defense response. Other indications that these behaviors are not based on access to food come from observations of wild-type females starved overnight on moistened filter paper and transferred back onto food. These females showed short head-to-head and head-to-side interactions, but did not show behavior resembling male courtship. Courting *retn* females, by contrast, primarily show posterior orientation (Fig. 3C,D), and will follow other females on and off a food source for minutes at a time.

Male-like behaviors in *retn* females are not dependent on *fru*

Genetic data indicate that males lacking *fru* M (P1 derived) transcripts show a ‘complete absence of sexual behavior’ (Anand et al., 2001). However, we observe male-like courtship by *retn* mutant females, which should lack *fru*M (Ryner et al., 1996). This suggests three possibilities: (1) *retn* mutants could lead to an up regulation of *fru*M in females; (2) there could be a very low level of *fru*M in wild-type and *retn* females, which, in the absence of *retn*, is sufficient to induce some male behavior; or (3) there could be an intrinsic, but weak, *fru*-independent pathway for male behavior that is repressed by *retn* or *retn*-expressing neurons (see Discussion for a model incorporating this idea). We have tested these possibilities.

As *fru*M RNA expression is male specific and is eliminated in females by TRA- and TRA2-mediated splicing of P1 transcripts into the *fru*F RNA form, we expect no increase in *fru*M in *retn* females. We addressed whether *retn* loss-of-function leads to upregulation of *fru*M in females. RT-PCR with one round of amplification using primers against *fru*M gave no detectable *fru*M product in Canton S or $retn^{-}$ mid-pupal or aged-adult female CNS tissue (data not shown). A second round of amplification showed an extremely low signal for *fru*M in equal amounts in both wild-type and $retn^{-}$ CNS tissue (data not shown). These results indicate that *fru*M is not upregulated in $retn^{-}$ CNS tissue, although the small amount of *fru*M detected in the second round of amplification might be responsible for the male-like behaviors in *retn* females.

We tested the dependence of the male-like behaviors in *retn* females upon the observed amount of *fru*M.$Df(3R)fru^{4\text{-}40}$ removes the P1 (responsible for transcripts under *tra*/*tra2* control) and P2 promoters, leaving the P3 and P4 promoters intact. $Df(3R)fru^{AJ96u3}$ removes P4 and the

entire *fru* protein coding region (Song et al., 2002). $fru^{4\text{-}40}/fru^{AJ96u3}$ flies lack P1 derived transcripts, but are healthy because of P3 and P4 activity (Song et al., 2002). RT-PCR analysis with two rounds of amplification upon CNS tissue from these females indicated a complete absence of *fru*F and *fru*M (data not shown), as expected. We tested for male-like behaviors by $retn^{-}; fru^{-}$ females ($retn^{z2\text{-}428}/retn^{dri8}; fru^{4\text{-}40}/fru^{AJ96u3}$). Such females aged for ~2.5 weeks, produced *retn*-like male behaviors (Fig. 3G,H), indicating an independence of such behaviors from *fru*M. In addition, similarly aged $retn^{-}$ females carrying a different *fru*M null allelic combination [$Df(3R)fru^{sat15}/Df(3R)fru^{4\text{-}40}$ (Anand et al., 2001)] also display substantial male-like courtship behavior (not shown). Taken together, these data indicate that the male-like behaviors observed in *retn* females are specified by a means independent of *fru*M.

retn does not alter male behaviors

We tested if *retn* alters male behaviors or functions. *retn* males court females, are not delayed in copulation (Fig. 4A), do not show significant courtship of other males (Fig. 4B) and have normal Muscles of Lawrence. *retn* males produce motile sperm and copulate normally, but show defects in sperm transfer and are partially sterile (L. M. Ditch, PhD thesis, University of California, 2002).

Sex matters in *retn* cells

To test if any *retn* cells have important sexual identities in males, we used *retn*-$Gal4^{89}$ to drive UAS-Tra^{F} in males. XY;*retn*-$Gal4^{89}$/UAS-Tra^{F} animals have male pigmentation patterns and sex combs, but genitalia are underdeveloped (data not shown; L. M. Ditch, PhD thesis, University of California, 2002). They court females with normal courtship indices, and court other males. Wild-type males do not court the *retn*-$Gal4^{89}$/UAS-Tra^{F} males (data not shown; L. M. Ditch, PhD thesis, University of California, 2002). These results indicate that, although *retn* mutations do not alter male behavior, some *retn*-$Gal4^{89}$-expressing cells have sex-specific identities essential for male sexual orientation.

Alternative splicing of *retn* transcripts does not show sex specificity

As *retn* has female-specific phenotypes, we asked if it is a direct target of regulation by Tra/Tra2-mediated alternative splicing focusing on central nervous system RNAs, as *retn* has non-sex-specific functions in other tissues (Gregory et al., 1996;Shandala et al., 1999;Shandala et al., 2002;Bradley et al., 2001;Iwaki et al., 2001). We analyzed RNA from the larval CNS, prior to the most sensitive period for sexual nervous system differentiation, and the early/mid pupal CNS, the primary period of sex-specific nervous system determination (Belote and Baker, 1987;Arthur et al., 1998).

retn has 12 exons, most of which are separated by small (fewer than 100 nucleotides) introns (Fig. 1). Exons 1 and 2, 4 and 6, and 6 and 7 are separated by large (multiple kb) introns, while exons 11 and 12 are separated by a 182 base intron. We used RT-PCR to analyze alternative processing between exons 1 and 4, 1 and 8 (pupal only), 4 and 8, 4 and 11 (pupal only), 8 and 11, and 8 and 12 (not shown). The data (Fig. 5) show the expected products, and two novel variants. None of these is sex-specific, which is completely consistent with the rescue of *retn* female behavioral (Fig. 3A,B) and egg-laying phenotypes using a common form cDNA.

The first novel form is rare (not visible inFig. 5A) relative to the previously described major RNA form, and joins exons 1 and 4, skipping exons 2 and 3. This creates an in frame deletion in the RNA, removing 318 bases and 106 amino acids, much of the N-terminal non-conserved region of the protein, but leaving the extended ARID box and C terminus intact. The second novel form is approximately equally abundant with the major form and joins exons 1 and 6, creating an in frame deletion removing 756 bases and 252 amino acids. This deletes from very near the protein start into the N-terminal region of the extended ARID box shared with the

mammalian Bright/Dril family of factors, leaving the C terminus intact. It is possible that this variant encodes the '95 kDa' form seen by Valentine et al. (Valentine et al., 1998).

retn is expressed in the CNS during pupal stages when sexual behavior is hardwired

To map *retn* expression in the CNS, we examined *retn*-driven GFP expression using *retn*-Gal4 insertions that rescue *retn* phenotypes with the *retn* cDNA. These Gal4 enhancer traps, in addition to rescuing *retn* viability and behaviors, exactly reproduce Retn antibody patterns in embryos and larval eye tissue (Shandala et al., 1999) (J. Sibbons, personal communication); therefore, they should represent the later CNS expression to a high degree of accuracy. Expression and projections were monitored using membrane-associated UAS-CD8::GFP (UAS-mGFP). *retn* expression in the CNS begins in the embryo (Gregory et al., 1996;Shandala et al., 2002), and continues through adulthood, in specific subsets of neurons. As we were primarily interested in neurons involved in adult behaviors, we focused on expression of *retn* in the periods before and during metamorphosis, when adult neurons are born and larval neurons are remodeled into adult-specific forms. Notably, we see expression in the mushroom bodies, subesophageal ganglion, ventral ganglion and developing photoreceptors. These patterns are essentially the same in both sexes.

Mushroom body (MB)—In the third instar, MB expression is seen in the Kenyon cell (KC) bodies lying in the dorsoposterior of the central brain, with staining in the calyx, containing KC dendrites, and the pedunculus and lobes, containing KC axons (Fig. 6D). Between 12 and 18 hours after puparium formation (APF), the calyx retracts, the α and β lobes narrow and what appears to be axonal debris can be seen at the lobe tips (arrow,Fig. 6E). At this stage there are slightly more *retn* cells in females than in males, perhaps reflecting the greater axon number in female MBs (Technau, 1984). By 36 hours APF, the adult α, α′, β, β′, and γ lobe projections are visible, although *retn* expression is stronger in α/β projections (Fig. 6F). Between 24 and 48 hours APF, expression in all lobes except α/β gradually fades, and by 48 hours only the α/β lobes can be seen. This pattern remains through the rest of metamorphosis.

Subesophageal ganglion (SOG)—In the larval SOG, two central groups of six or seven neurons and two anterior groups of five neurons send projections towards the protocerebrum and ventral nerve cord (Fig. 6G). Laterally to these neurons are four additional neurons per side. The projections of these neurons form a dense pattern, and individual projections cannot be discerned. Retraction of larval-specific processes can be seen beginning six hours APF (Fig. 6H, 18 hours APF); by 36 hours APF, new processes are evident. The number of SOG neurons expressing *retn* remains constant, but projections become increasingly dense (Fig. 6I, 48 hours APF) through the pupal period (seeFig. 6C).

Ventral ganglion—In the larval ventral nerve cord (VNC), 18 paired dorsal lateral neurons, nine per side, send projections towards the midline (Fig. 6J). These may mediate signaling to or from the nine larval abdominal segments. By 24 hours APF, the abdominal neurons are now six pairs, residing at the abdominal tip (Fig. 6K). Beyond 36 hours APF and continuing into adulthood, three sets of paired abdominal neurons are visible (Fig. 6L). These final neurons may project outwards from the CNS. A small subset of adult peripheral sensory neurons that innervate the female reproductive structures also send their projections into the terminal abdominal ganglion (data not shown).

Eye—*retn*-Gal4^{89} is expressed posterior to the morphogenetic furrow, in photoreceptor cells R1-R6, which project to the lamina and R8, which projects to the medulla (not shown), as is also seen with Retn antibody staining (J. Sibbons, personal communication). Beyond 48 hours APF, R8 expression and projections fade, although lamina projections remain (48 hour pupal

eye,Fig. 7J). Expression in the eye, MB, SOG and ventral nerve cord is still visible post-eclosion (Fig. 6C, early adult).

retn affects axon guidance in mushroom bodies

We observed MB-specific abnormalities in three different *retn* mutant genotypes: *retn*-Gal4^{89}/*retn*$^{Z2\text{-}428}$ larvae and pupae; *retn*^{dri8}/*retn*$^{Z2\text{-}428}$, and *retn*^{Ro44}/*retn*^{RO44} adults (Fig. 7B,C,E) MB neurons diverge within the nerve tracks and β-lobe neurons cross the midline and join with the opposite β-lobe neurons, causing β-lobe fusion, compared with *retn*-Gal4^{89}/+. This is more common in females than males (4/10 larval females, 0/11 larval males, 7/12 pupal females, 2/19 pupal males for *retn*-Gal4^{89}/*retn*$^{Z2\text{-}428}$), but phenotypes of *retn; fru* males (not shown) indicate that *retn* functions in male neurons. Using antibodies to Fas2, which is expressed in MB axons projecting to the α- and β-lobes in *retn*^{dri8}/*retn*$^{Z2\text{-}428}$ and *retn*^{R044}/*retn*^{R044} adults, we found that in a subset of mutant (4/6 *retn*^{dri8}/*retn*$^{Z2\text{-}428}$ and 1/3 *retn*^{RO44}/*retn*^{RO44}) females, axons in the posterior part of the β-lobe crossed the midline, leading to β-lobe fusion (Crittenden et al., 1998). In addition, in those animals with β-lobe fusion, there were fewer Fas2-positive axons in the β-lobe. These MB fusion phenotypes are similar to the β-lobe fusion phenotypes reported in other mutants, such as *linotte/derailed*, *Drosophila fragile X mental retardation 1*, *fused lobes*, *ciboulot* and *α-lobe absent* (Moreau-Fauvargue et al., 1998; Boquet et al., 2000;Michel et al., 2004). Resistance is shown by the vast majority of females of these genotypes, thus MB fusion is unlikely to be causal for resistance.

Neuronal birthdates and pathfinding errors in mutant clones

To determine *retn* neuronal birth dates and the neural phenotypes of *dri*-class alleles, we used the MARCM system (Lee and Luo, 1999), which can simultaneously create homozygous mutant cells and allow them to express Gal4-regulated marker genes. *retn*-expressing MB neurons are born throughout the larval and pupal stages and eye clones appear at all embryonic and larval stages. The VNC neurons are born only within 48 hours of egg laying, and SOG *retn* neurons are born in 8-hour-old or younger embryos.

Homozygous *retn*-Gal4^{89} clones show striking mis-projection phenotypes in SOG neurons. The normal elaboration and symmetry of arbors in mid-pupae is diminished; ventral dendritic branches do not show normal density (compare arrowhead in Fig. 7F with arrowhead in Fig. 7G), and anterior projections wander and fail to extend (compare arrows in Fig. 7F and Fig. 7G). Neurons also fail to fasciculate normally. A central SOG midline-crossing tract, visible throughout metamorphosis, contains tightly bundled projections (arrow, Fig. 7H). In mutant clones, projections stray from this tract, apparently losing some adherent ability (arrow, Fig. 7I). Photoreceptor neurons also mis-project. In *retn*^{dri} clones, induced in the embryo, R1-R6 cells overshoot the lamina, and a number now target the medulla (ME, arrows; Fig. 7J, wild type; Fig. 7K, mutant). Although *retn* mutations alter neuronal projection patterns, and projection differences are consistent with changes in behavior, we have not yet mapped *retn* behavioral functions to a particular set of neurons, nor have we demonstrated that the projection differences, as opposed, for example, to *retn*-induced reductions in neural activity, are responsible for behavioral changes.

Discussion

Behavior: *retn*, *dsf* and *fru*

retn functions in multiple, separable processes during development. It acts in differentiation and control of gene expression along the anterior posterior and dorsal ventral axes in embryos (Shandala et al., 1999;Valentine et al., 1998). It also acts in the production of various tube structures such as salivary ducts and gut (Bradley et al., 2001;Iwaki et al., 2001). Failures in these or other embryonic processes with *dri*-class (null or near null) alleles lead to embryonic

death. *retn*-class (hypomorphic missense) alleles can perform the embryonic functions but show defects in neural development and projections. Correlating with this are changes in female behavior, including resistance to male courtship and, strikingly, generation of male-like courtship behaviors. Additional functions in development of internal genital ducts and fertility have been observed (L. M. D., B. J. T. and M. M., unpublished) and will be discussed elsewhere.

retn neural and behavioral phenotypes are substantially different from those of *dsf* or *fru. dsf* females, like *retn*-females, are sterile and resist male courtship (Finley et al., 1997). For *dsf*, sterility results from loss of motor synapses on the circular muscles of the uterus (Finley et al., 1997). By contrast, these synapses are intact in *retn* females. *dsf* females show no male behaviors (Finley et al., 1997), while *retn* females do. *dsf* males are bisexual and slow to copulate, owing to inefficient abdominal bending, correlated with abnormal synapses on the muscles of ventral abdominal segment 5 (Finley et al., 1997). *retn* males court and mate with normal kinetics and have normal A5 synapses. This suggests that *retn* and *dsf* have largely separate functions.

retn and *fru* also have different phenotypes. In a wild-type background *retn* behavioral phenotypes are restricted to females. *fru* behavioral phenotypes are restricted to males and include failure to attempt copulation, bisexual and homosexual courtship, and, in the strongest allelic combinations, complete lack of male courtship. In addition, *fru* males lack the male-specific muscles of Lawrence in dorsal abdominal segment 5. *retn* males have normal muscles of Lawrence, and *retn* females do not have muscles of Lawrence. In addition, the larval and pupal expression patterns of *retn* (this paper) and the sex-specific products of the *fru* P1 promoter (Lee et al., 2000), notably the active male-specific *fru* proteins, show little or no overlap. This all suggests that *fru* and *retn* are unlikely to interact intracellularly and would be expected to be involved in different aspects of behavioral control.

The latter conclusion seems to be contradicted by the male-like courtship generated by *retn* females, as previous work demonstrates that otherwise wild-type males require FRU-M to generate male behavior (Anand et al., 2001). We have operationally and molecularly shown that the male behavior generated by *retn* females occurs even in the absence of *fru* P1 transcripts (Fig. 3G,H).

A model for the roles of *fru* and *retn* in male sexual behavior

We have developed a plausible working model that reconciles the data on the necessity of *fru*M in males and male-like courtship by *retn* females. The largely non-overlapping expression patterns of *fru* and *retn* suggests that the formal interactions of this model will result from interactions between networks of *fru*- and *retn*-influenced neurons rather than by intracellular regulatory interactions involving FRU-M and RETN, although the model can accommodate either situation.

Our model posits that in the absence of *fru*M and *retn* the nervous system has an inherent tendency to set down some rudiments of neural pathways for male courtship behavior (Fig. 8A).

When *retn* is wild type and *fru*M is not expressed, as in wild-type females, *retn*, or cells expressing *retn* [perhaps in conjunction or parallel with other factors such as *dsx*F (below)], act to suppress the basal male courtship pathway (Fig. 8B). This blocks male courtship behaviors. This is the case in wild-type females, as shown.

Finally, in wild-type males, *fru*M or cells expressing *fru*M, perhaps along with other factors such as *dsx*M, act to strengthen the male courtship pathway such that the repressive action of *retn*-expressing cells is overpowered (Fig. 8C). This makes *fru* the switch that results in male

behavior and captures both the requirement for fru^+ in males, and the male-like courtship by *retn* females.

This model does not rule out involvement of other components. For example, work by Waterbury et al. (Waterbury et al., 1999) suggests that *dsx*F can suppress male behaviors in a $retn^+$ background. This can be fitted into the model as an additional female-specific block to male behavior in both Fig. 8A and 8B. A simple prediction of such a role for *dsx* is that reduction of *dsx* expression in a *retn* mutant background will enhance the *retn* phenotype. Recent work involving expression of *fru* RNAi in a subset of *fru* neurons suggests a role for temporally repression in the sequencing of male behaviors in courtship (Manoli and Baker, 2004).

An extensive series of experiments is in progress to test predictions of this model. Experiments are also in progress to determine if *dsx* participation fits within the context of the model, and to identify the molecules and mechanisms downstream of *retn* in the control of behavior.

Acknowledgements

We thank Erin Gross and Michael Benedetti for substantial effort in the genetic screen yielding *retn*, Rebecca Wagaman for work mapping the exon 1-6 splice form of *retn* RNA, and Michael Ludwig for technical assistance. This work was supported by grants from the NIH (MH57460) and NSF (IBN-0315660) to M.McK. and from the NIH (GM-56920, NS033352) to B.J.T. J.L.P. was supported by an American Cancer Society Postdoctoral Fellowship (PF-00-324-01-DDC), while K.D.F. was supported by an National Institute of Neurological Diseases and Stroke Postdoctoral Fellowship. T.S. is currently an NIH Predoctoral Trainee (GM07601).

References

Altschul SF, Gish W, Miller W, Myers EW, Lipman DJ. Basic local alignment search tool. J Mol Biol 1990;215:403–410. [PubMed: 2231712]

Anand A, Villela A, Ryner LC, Carlo T, Goodwin SF, Song HJ, Gailey DA, Morales A, Hall JC, Baker BS, Taylor BJ. Molecular genetic dissection of the sex-specific and vital functions of the *Drosophila melanogaster* sex determination gene *fruitless*. Genetics 2001;158:1569–1595. [PubMed: 11514448]

Arthur BI Jr, Jallon JM, Caflisch B, Choffat Y, Nothinger R. Sexual behavior is irreversibly programmed during a critical period. Curr Biol 1998;8:1187–1190. [PubMed: 9799737]

Belote JM, Baker BS. Sexual behavior: its genetic control during development and adulthood in *Drosophila melanogaster*. Proc Natl Acad Sci USA 1987;84:8026–8030. [PubMed: 3120181]

Boquet I, Hitier R, Dumas M, Chaminade M, Preát T. Central brain postembryonic development in *Drosophila:* implication of genes expressed at the interhemispheric junction. J Neurobiol 2000;42:33–48. [PubMed: 10623899]

Bradley PL, Haberman AS, Andrew DJ. Organ formation in *Drosophila*: specification and morphogenesis of the salivary gland. Bioessays 2001;23:901–911. [PubMed: 11598957]

Brand AH, Perrimon N. Targeted gene expression as a means of altering cell fates and generating dominant phenotypes. Development 1993;118:401–415. [PubMed: 8223268]

Christiansen AE, Keisman EL, Ahmad SM, Baker BS. Sex comes in from the cold: the integration of sex and pattern. Trends Genet 2002;18:510–517. [PubMed: 12350340]

Crittenden JR, Skoulakis EMC, Han KA, Kalderon D, Davis RL. Tripartite mushroom body architecture revealed by antigenic markers. Learn Mem 1998;5:38–51. [PubMed: 10454371]

Finley KD, Taylor BJ, Milstein M, McKeown M. *dissatisfaction*, a gene involved in sex-specific behavior and neural development of *Drosophila melanogaster*. Proc Natl Acad Sci USA 1997;94:913–918. [PubMed: 9023356]

Finley KD, Edeen PT, Foss M, Gross E, Ghbeish N, Palmer RH, Taylor BJ, McKeown M. *dissatisfaction* encodes a Tailless-like nuclear receptor expressed in a limited subset of CNS neurons controlling *Drosophila* sexual behavior. Neuron 1998;21:1363–1374. [PubMed: 9883729]

Gailey DA, Taylor BJ, Hall JC. Elements of the *fruitless* locus regulate development of the muscle of Lawrence, a male-specific structure in the abdomen of *Drosophila melanogaster* adults. Development 1991;113:879–890. [PubMed: 1821857]

Goodwin SF. Molecular neurogenetics of sexual differentiation and behavior. Curr Opin Neurobiol 1999;9:759–765. [PubMed: 10607639]

Greenspan RJ, Ferveur JF. Courtship in *Drosophila*. Annu Rev Genet 2000;34:205–232. [PubMed: 11092827]

Gregory SL, Kortschak RD, Kalionis W, Saint R. Characterization of the *dead ringer* gene identifies a novel, highly conserved family of sequence-specific DNA-binding proteins. Mol Cell Biol 1996;16:792–799. [PubMed: 8622680]

Hall JC. The mating of a fly. Science 1994;264:1702–1714. [PubMed: 8209251]

Ito H, Fujitani K, Usui K, Shimizu-Nishikawa K, Tanaka S, Yamamoto D. Sexual orientation in *Drosophila* is altered by the satori mutation in the sex-determination gene *fruitless* that encodes a zinc finger protein with a BTB domain. Proc Natl Acad Sci USA 1996;93:9687–9692. [PubMed: 8790392]

Iwahara J, Iwahara M, Daughdrill GW, Ford J, Clubb RT. The structure of the *Dead ringer*-DNA complex reveals how AT-rich interaction domains (ARIDs) recognize DNA. EMBO J 2002;21:1–13. [PubMed: 11782420]

Iwaki DD, Johansen KA, Singer JB, Lengyel JA. *drumstick*, *bowl*, and *lines* are required for patterning and cell rearrangement in the *Drosophila* embryonic hindgut. Dev Biol 2001;240:611–626. [PubMed: 11784087]

Kaelin WG Jr, Krek W, Sellers WR, DeCaprio JA, Ajchenbaum F, Fuchs CS, Chittenden T, Li Y, Farnham PJ, Blanar MA. Expression cloning of a cDNA encoding a retinoblastoma-binding protein with E2F-like properties. Cell 1992;70:351–364. [PubMed: 1638635]

Lee G, Foss M, Goodwin SF, Carlo T, Taylor BT, Hall JC. Spatial, temporal, and sexually dimorphic expression patterns of the *fruitless* gene in the *Drosophila* central nervous system. J Neurobiol 2000;43:404–426. [PubMed: 10861565]

Lee T, Luo L. Mosaic analysis with a repressible cell marker for studies of gene function in neuronal morphogenesis. Neuron 1999;22:451–461. [PubMed: 10197526]

Manoli DS, Baker BS. Median bundle neurons coordinate behaviours during Drosophila male courtship. Nature 2004;430:564–569. [PubMed: 15282607]

Michel CI, Kraft R, Restifo LL. Defective neuronal development in the mushroom bodies of *Drosophila fragile X mental retardation 1* mutants. J Neurosci 2004;24:5789–5809. [PubMed: 15215301]

Moreau-Fauvarque C, Taillebourg E, Boissoneau E, Mesnard J, Dura J-M. The receptor tyrosine kinase gene *linotte* is required for neuronal pathway selection in the *Drosophila* mushroom bodies. Mech Dev 1998;78:47–61. [PubMed: 9858681]

O'Kane CJ, Asztalos Z. Sexual behavior: courting dissatisfaction. Curr Biol 1999;9:R289–R292. [PubMed: 10226020]

Pearson WR, Lipman DJ. Improved tools for biological sequence comparison. Proc Natl Acad Sci USA 1988;85:2444–2448. [PubMed: 3162770]

Pitman JL, Tsai CC, Edeen PT, Finley KD, Evans RM, McKeown M. DSF nuclear receptor acts as a repressor in culture and in vivo. Dev Biol 2002;245:315–328. [PubMed: 11977984]

Ryner LC, Goodwin SF, Castrillon DH, Anand A, Villella A, Baker BS, Hall JC, Taylor BJ, Wasserman SA. Control of male sexual behavior and sexual orientation in *Drosophila* by the *fruitless* gene. Cell 1996;87:1079–1089. [PubMed: 8978612]

Schupbach T, Wieschaus E. Female sterile mutations on the second chromosome of *Drosophila melanogaster*. II. Mutations blocking oogenesis or altering egg morphology. Genetics 1991;129:1119–1136. [PubMed: 1783295]

Shandala T, Kortschak RD, Gregory S, Saint R. The *Drosophila dead ringer* gene is required for early embryonic patterning through regulation of argos and buttonhead expression. Development 1999;126:4341–4349. [PubMed: 10477301]

Shandala T, Kortschak RD, Saint R. The *Drosophila retained*/ *dead ringer* gene and ARID gene family function during development. Int J Dev Biol 2002;46:1–8.

Song HJ, Billeter JC, Reynaud E, Carlo T, Spana EP, Perrimon N, Goodwin SF, Baker BS, Taylor BJ. The *fruitless* gene is required for the proper formation of axonal tracts in the embryonic central nervous system of Drosophila. Genetics 2002;162:1703–1724. [PubMed: 12524343]

Technau GM. Fiber number in the mushroom bodies of adult Drosophila melanogaster depends on age, sex, and experience. J Neurogenet 1984;1:113–126. [PubMed: 6085635]

Ueda A, Kidokoro Y. Aggressive behaviors of female *Drosophila melanogaster* are influenced by their social experience and food resources. Physiol Entomol 2002;27:21–28.

Valentine SA, Chen G, Shandala T, Fernandez J, Mische S, Saint R, Courey AJ. Dorsal-mediated repression requires the formation of a multiprotein repression complex at the ventral silencer. Mol Cell Biol 1998;18:6584–6594. [PubMed: 9774673]

Villella A, Hall JC. Courtship anomalies caused by *doublesex* mutations in *Drosophila melanogaster*. Genetics 1996;143:331–344. [PubMed: 8722785]

Villella A, Gailey DA, Berwald B, Ohshima S, Barnes PT, Hall J. Extended reproductive roles of the *fruitless* gene in *Drosophila melanogaster* revealed by behavioral analysis of new *fru* mutants. Genetics 1997;147:1107–1130. [PubMed: 9383056]

Waterbury JA, Jackson LJ, Schedl P. Analysis of the doublesex female protein in *Drosophila melanogaster*: role in sexual differentiation and behavior and dependence on intersex. Genetics 1999;152:1653–1667. [PubMed: 10430590]

Yamamoto D, Jallon JM, Komatsu A. Genetic dissection of sexual behavior in *Drosophila melanogaster*. Annu Rev Entomol 1997;42:551–585. [PubMed: 9017901]

Yamamoto D, Fujitani K, Usui K, Ito H, Nakano Y. From behavior to development: genes for sexual behavior define the neuronal sexual switch in *Drosophila*. Mech Dev 1998;73:135–146. [PubMed: 9622612]

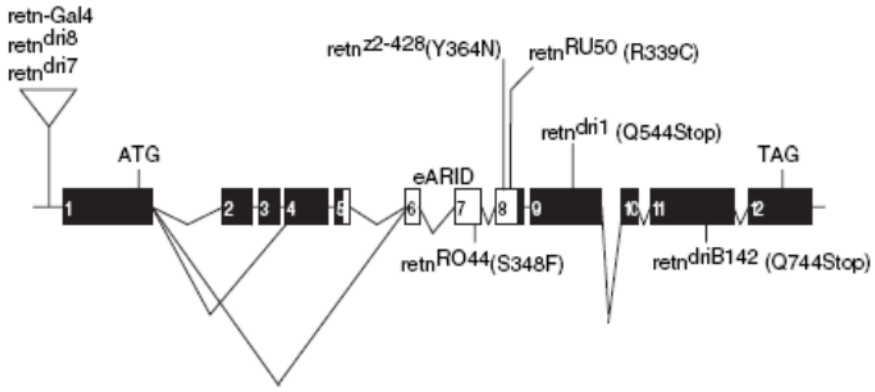

Fig 1. Mutations and structure of the *retn* gene

The structure of the *retn* gene is shown (introns not to scale), including the previously undetected exon 1-4 and exon 1-6 splice variants. Positions and structures derived from Gregory et al. (Gregory et al., 1996) and from our analysis of the genomic sequence of the region. The regions shown in white encode the extended ARID box DNA-binding domain. The viable ('*retn* class') alleles $retn^{RO44}$, $retn^{z2\text{-}428}$ and $retn^{RU50}$ encode missense mutations within the ARID box. Embryonic lethal ('*dri* class') alleles $retn^{dri1}$ and $retn^{driB142}$ encode nonsense mutations. P-element insertions $retn^{dri7}$ and $retn^{dri8}$ map in or near *retn* exon 1. *retn*-Gal4 insertions were created by targeted transposition into the $retn^{dri7}$ and $retn^{dri8}$ positions (Shandala et al., 1999).

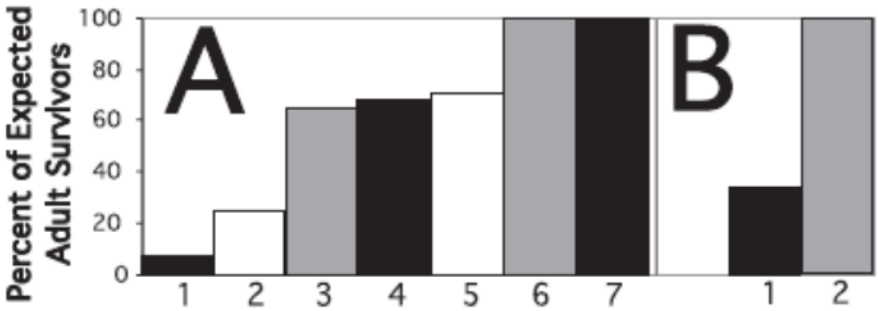

Fig 2. *retn* mutations affect viability

(A) Eclosion rates for *retn* heteroallelic combinations. $retn^{z2\text{-}428}/retn^{dri2}$ (1) and $retn^{z2\text{-}428}/retn^{dri1}$ (2) offspring eclose with 8% and 25% of expected rates; $retn^{RU50}/retn^{dri2}$ (3) and $retn^{RU50}/retn^{dri1}$ (4) eclose with 65% and 68% of expected numbers; $retn^{z2\text{-}428}/retn^{dri8}$ (5) and $retn^{RU50}/retn^{dri8}$ (6) eclose with 71% and 100% of expected numbers. $retn^{z2\text{-}428}/retn^{RU50}$ (7) is completely viable. (B) *retn* cDNA rescues partial lethality of *retn*-Gal4/$retn^{z2\text{-}428}$. *retn*-$Gal4^{89}/retn^{z2\text{-}428}$; +/+ trans-heterozygotes (1) eclose with 33% of expected numbers, while *retn*-$Gal4^{89}/retn^{z2\text{-}428}$; UAS-*retn*/+ individuals (2) eclose at 100% of expected rates.

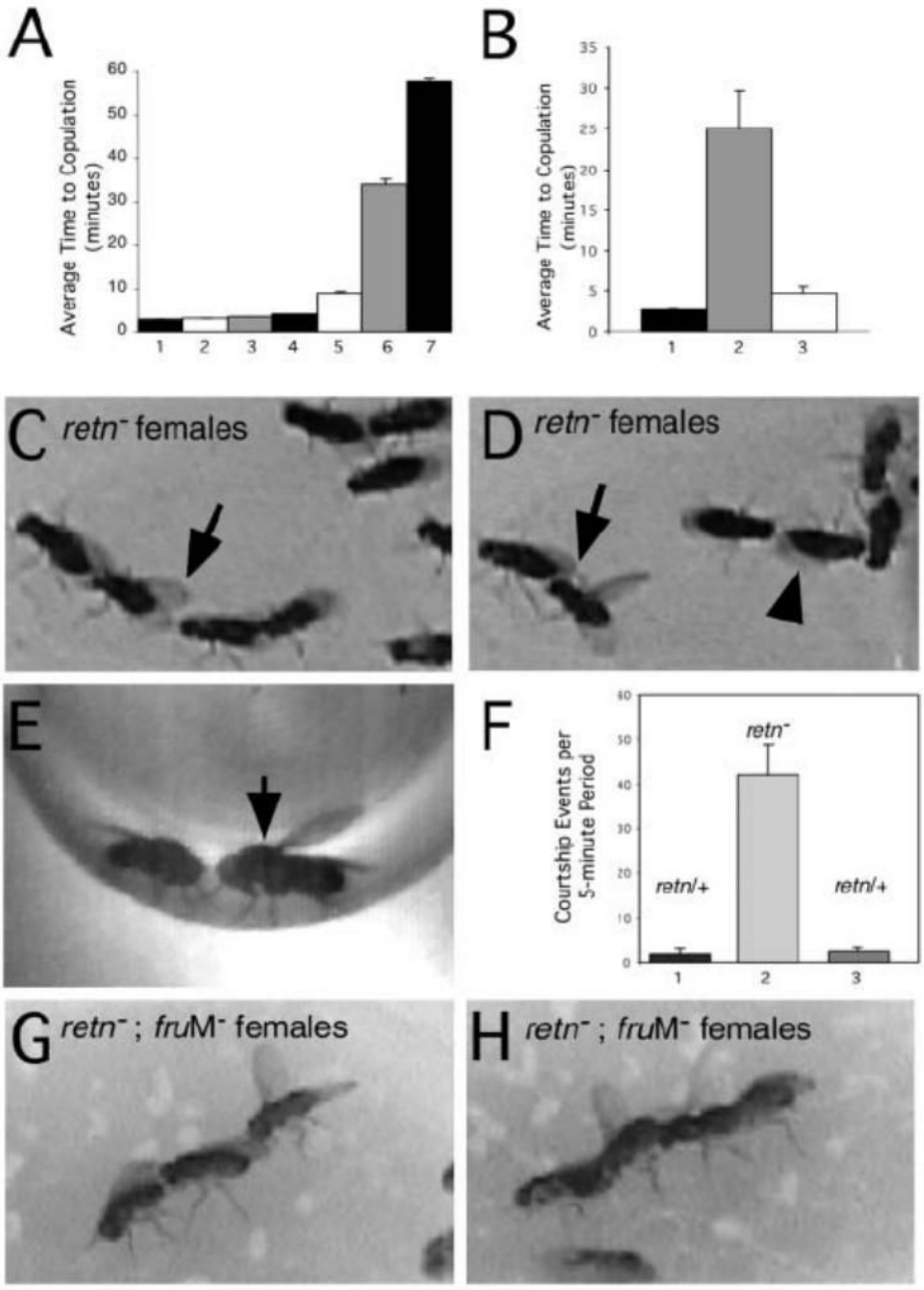

Fig 3. *retn* female behaviors

(A) *retn* female resistance to male courtship increases with allelic strength. (1) Wild type (Canton-S) (CS), (2) $retn^{dri2}$/+, (3) $retn^{RU50}$/+, (4) $retn^{z2\text{-}428}$/+, (5) $retn^{z2\text{-}428}/retn^{RU50}$, (6) $retn^{RU50}/retn^{dri2}$, (7) $retn^{z2\text{-}428}/retn^{dri2}$. Average time of courtship prior to copulation for 20 females per genotype is shown. Error bars indicate s.e.m. Resistance behavior to a maximum of 1 hour was measured. Wild-type females (1), and $retn^{dri2}$/+ (2), $retn^{RU50}$/+ (3) and $retn^{z2\text{-}428}$/+ females (4) copulate in 2-4 minutes ($P>0.05$ relative to wild type). $retn^{RU50}/retn^{z2\text{-}428}$ females (5) average 8.8 minutes ($P=0.013$). $retn^{RU50}/retn^{dri2}$ females (6) average 34 minutes ($P=5\times10^{-5}$), and $retn^{z2\text{-}428}/retn^{dri2}$ (7) females average 58 minutes ($P=5\times10^{-17}$). (B) *retn* cDNA rescues female resistance behavior. (1)Wild type (CS), (2) *retn*-$Gal4^{89}/retn^{RU50}$;

+/+, (3) *retn*-Gal4^{89}/*retn*^{RU50}; UAS-*retn*/+.*retn*-Gal4^{89}/*retn*^{RU50}; +/+ females resist courtship for an average of 25 minutes ($P=4\times10^{-5}$ relative to wild type). *retn*-Gal4^{89}/*retn*^{RU50}; UAS-*retn*/+ females copulate in 4.8 minutes ($P=3\times10^{-4}$ compared with mutant without construct), comparable with wild type ($P=0.077$). (C) Courtship chain of *retn* (*retn*$^{z2\text{-}428}$/*retn*^{dri8}) females (arrow). (D) Female wing extension performed at another female (arrow). Additional chaining can be seen towards the right (arrowhead). (E) Female (arrow) extends wing at courting male. (F) Bisexual behavior is increased in *retn* females. (1) *retn*$^{z2\text{-}428}$/+, (2) *retn*$^{z2\text{-}428}$/*retn*^{dri8}, (3) *retn*^{dri8}/+.*retn*^{dri8}/+ and *retn*$^{z2\text{-}428}$/+ females average fewer than three courtship-like behaviors per observation period. *retn*$^{z2\text{-}428}$/*retn*^{dri8} females average 42±7 courtship events ($P=0.0001$ relative to controls). (G,H) *retn*$^{z2\text{-}428}$/*retn*^{dri8}; *fru*$^{4\text{-}40}$/*fru*^{AJ96u3} females generate male-like courtship, including both following behavior and wing extension.

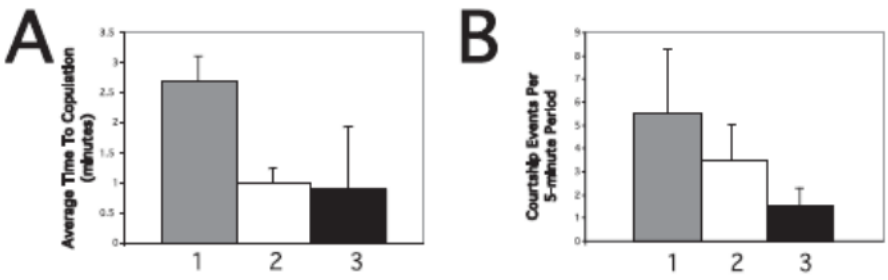

Fig 4. Courtship behaviors in *retn* males

(A,B), (1) Wild type (CS), (2) *retn*$^{z2\text{-}428}$/*retn*^{RU50}, (3) *retn*$^{z2\text{-}428}$/*retn*^{dri8}. (A) *retn* male courtship of females is comparable with wild type. CS males copulate on average 2.7±0.4 minute after initiation of courtship; *retn*$^{z2\text{-}428}$/*retn*^{RU50} males copulate on average in 1.0±0.3 minutes (P=0.1 relative to CS); *retn*$^{z2\text{-}428}$/*retn*^{dri8} males average 0.9±1.0 minutes (P=0.05 relative to CS). (B) *retn* males show low levels of bisexual courtship, comparable with wild-type bisexual courtship. CS males average 5.5±2.8 male-by-male courtship events per 5-minute observation period; *retn*$^{z2\text{-}428}$/*retn*^{RU50} males average 5.5±2.6 courtship events (P=1 relative to CS); *retn*$^{z2\text{-}428}$/*retn*^{dri8} males average 1.5±0.8 events (P=0.2).

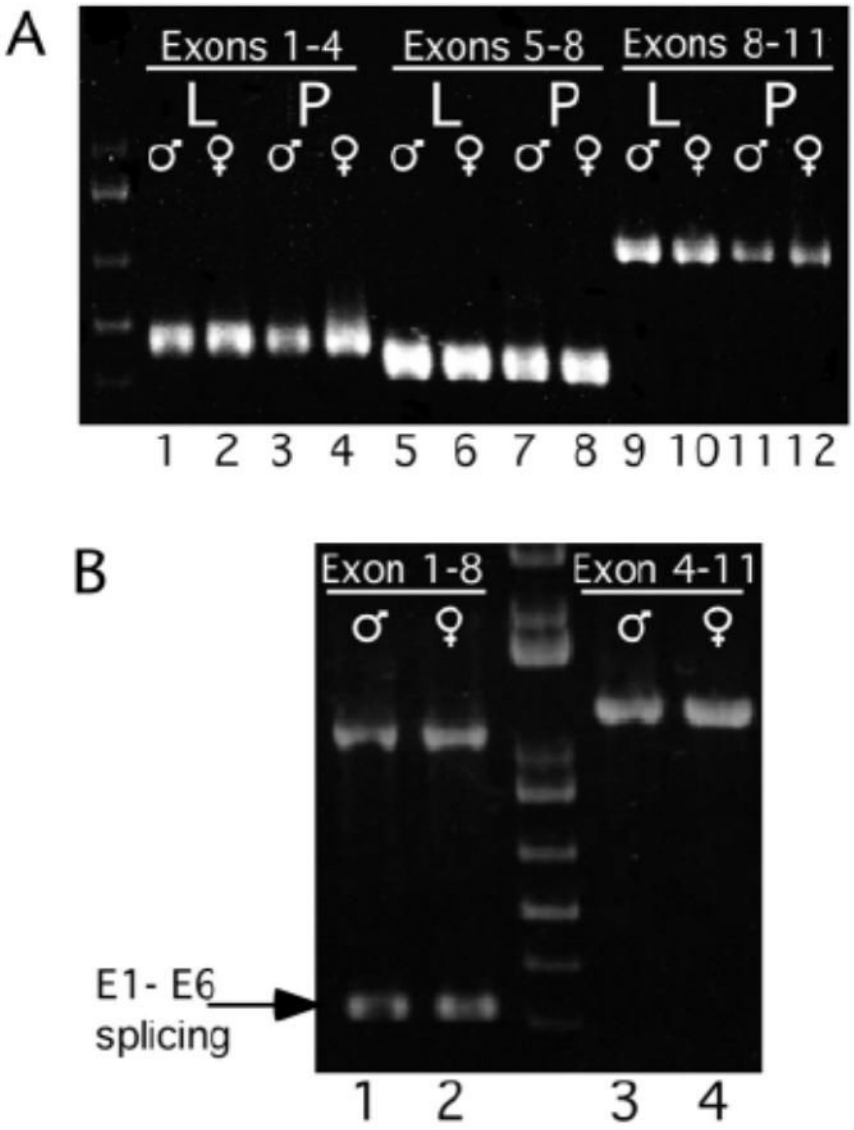

Fig 5. Sex-non-specific alternative splicing of *retn*

(A) A lack of sex-specific splicing of *retn*. RNAs from CNS tissue from late third instar larvae (lanes 1, 2, 5, 6, 9, 10) and mid-stage pupae (lanes 3, 4, 7, 8, 11, 12) from both sexes were analyzed by RT-PCR probing exons 1 to 4 (lanes 1 to 4), 4 to 8 (lanes 5 to 8), and 8 to 11 (lanes 9 to 12). The splice variant of *retn* joining exon 1 to 4 is present at very low levels and migrates beyond the level shown. (B) An abundant splice variant of *retn* joining exon 1 to 6 is present in both sexes. RNAs from CNS tissue from mid-stage pupae of both sexes were analyzed as above (A), probing between exons 1 and 8 (lanes 1 and 2), and 4 and 11 (lanes 3 and 4). The faster migrating band in lanes 1 and 2 represent splice variant 1-6.

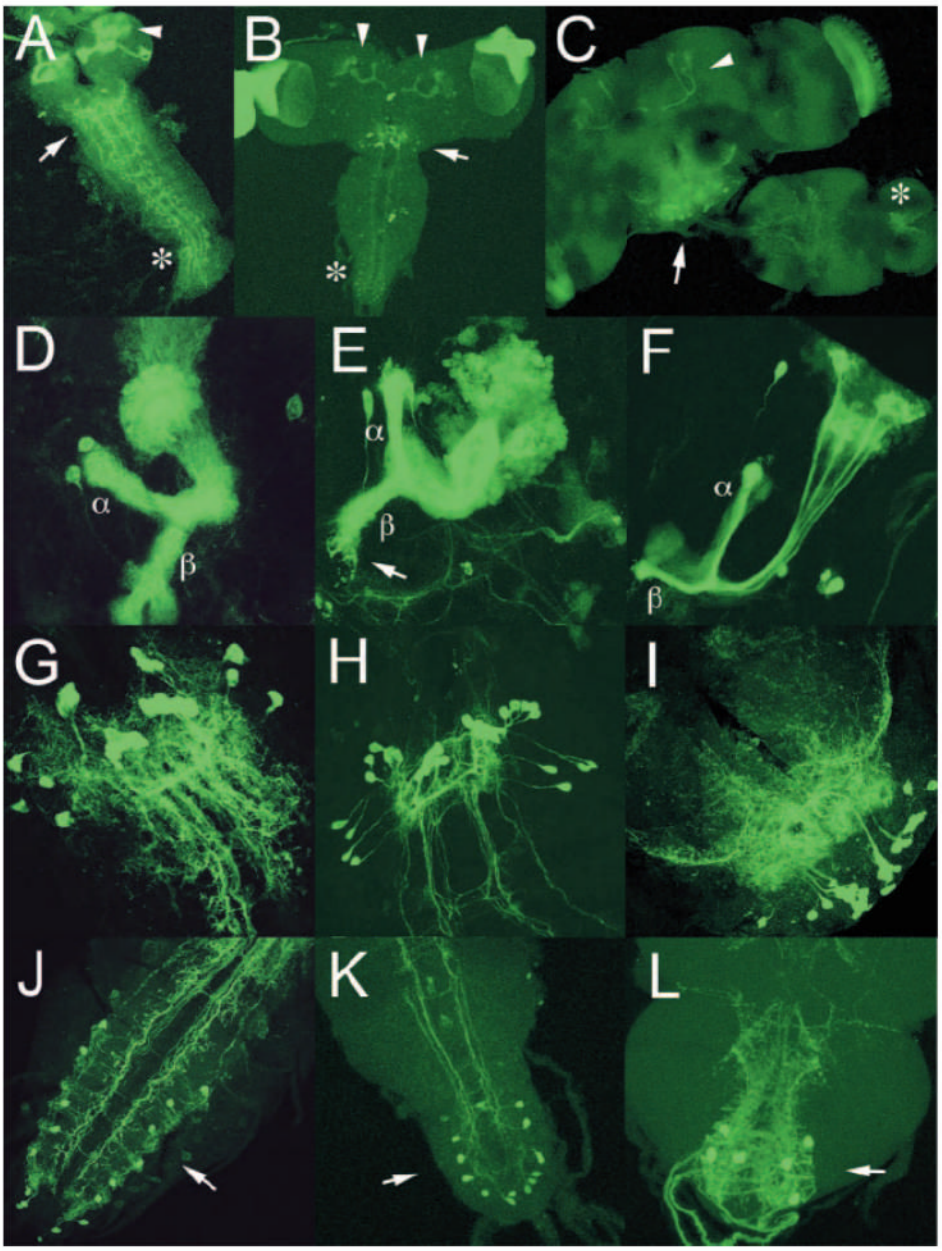

Fig 6. *retn* expression during metamorphosis

retn-Gal4/+; UAS-mGFP expression in late larval (A,D,G,J), early pupal (B,E,H,K), and late pupal/early adult (C,F,I,L) stages. (A-L) Anterior is upwards. (A-C) *retn* expression labels subsets of CNS neurons through metamorphosis: mushroom bodies (arrowheads), subesophageal ganglion (arrows) and ventral abdominal ganglion (asterisks). (D-F) *retn* labels α and β smushroom body processes in the larval CNS (D). These projections are pruned in 24-hour-old pupae (arrow in E). In 48-hour-old pupae, expression can be seen in all MB lobes, but expression subsequently fades in non- α/β projecting neurons (F). (G-I) Subesophageal ganglion cells remain constant in number, but show remodeling of projections from larval (G) to early (H) and late (I) pupal patterns. (J-L) Eighteen larval *retn*-expressing abdominal ganglion cells (arrow, J) reduce to 12 in early pupae (arrow, K). Six neurons are present (arrow, L) in late pupal stages.

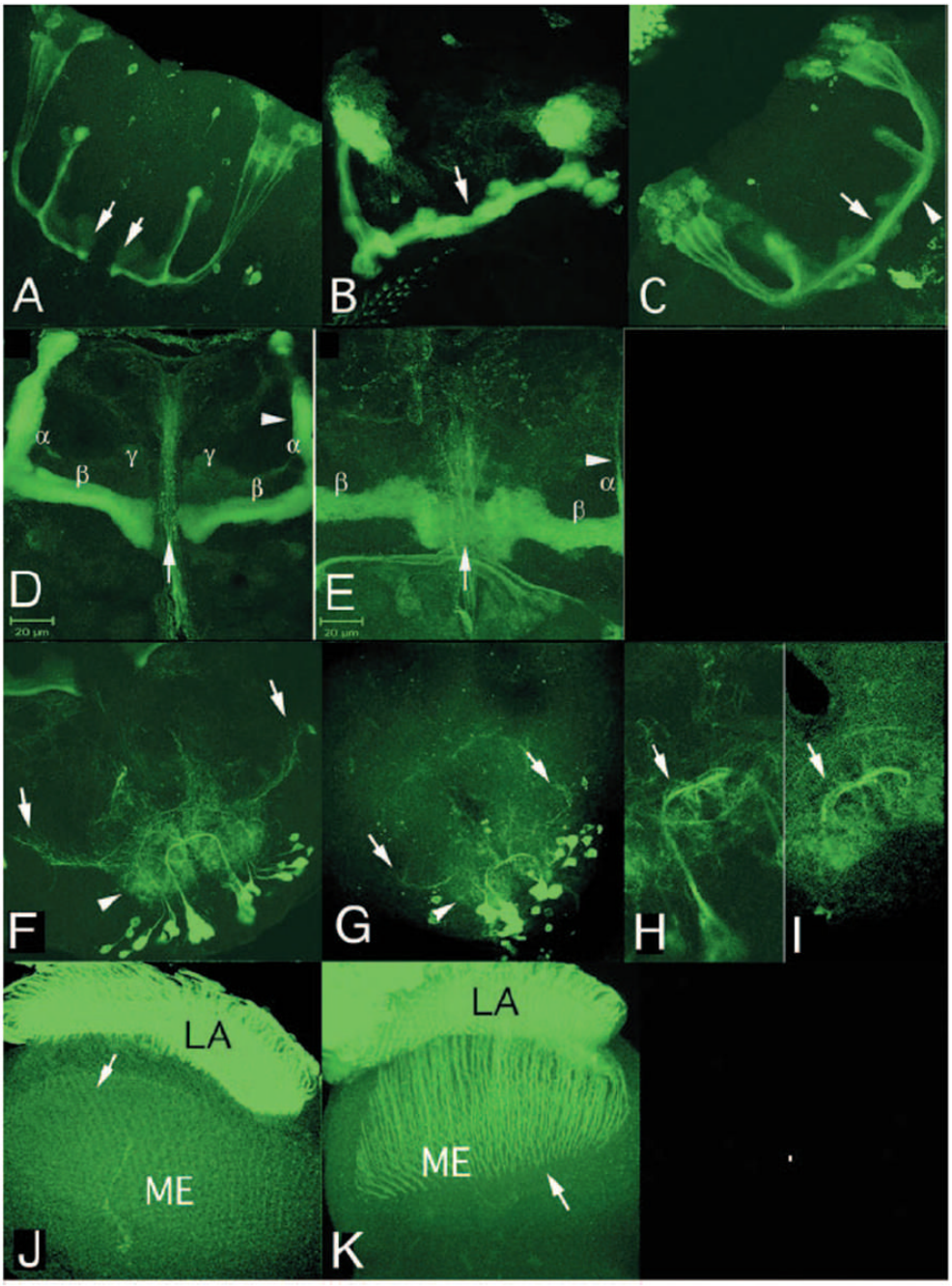

Fig 7. *retn* mutations cause neuronal pathfinding errors

(A) Mushroom bodies in *retn*-Gal4^{89}/+ show a clear separation of β-lobes (arrows). (B) In *retn*-Gal4^{89}/*retn*$^{z2\text{-}428}$ larvae, β-lobe fusion is evident (arrow). Compare with single larval MB in Fig. 6D, which is unlinked to its paired MB. (C) *retn*-Gal4^{89}/*retn*$^{z2\text{-}428}$ pupae also show β-lobe fusion (arrow) and poor fasciculation of neuronal projections (arrowhead). (D) β slobes of Canton-S adult female brain do not cross the midline. In 90% (*n*=6) Canton-S adult male brains there was no lobe fusion but one animal did have some crossing β-lobe fibers; a low frequency of β-lobe fiber crossing has been noted in wild-type animals (Moreau-Fauvarque et al., 1998;Michel et al., 2004). The gamma lobe fibers label weakly with Fas2 (Crittenden et al., 1998). Arrow and arrowhead indicate the midline between the β-lobes and the β-lobe,

respectively. (E) β-Lobes of *retn*^{dri8}/*retn*$^{z2\text{-}428}$ adult female have Fas2-positive axons that cross the midline giving a fused appearance. In this mutant female, the right α-lobe is also smaller than in wild-type females, as though there are fewer Fas2-postive axons. β-Lobe fusion of Fas2-positive axons was also found in 75% (*n*=4) of *retn*^{dri8}/*retn*$^{z2\text{-}428}$ and 33% (*n*=3) of *retn*^{RO44}/*retn*^{RO44} adult male brains. Anterior is upwards. Arrow and arrowhead indicate the midline between the β-lobes and the β-lobe, respectively. (F,H,J) *retn*-Gal4^{89}/+; UAS-mGFP. (G,I,K) FRTG13, *retn*-Gal4^{89}/FRTG13, *retn*-Gal4^{89}; UAS-mGFP clones following heat shock of hs-FLP; FRTG13, *retn*-Gal4^{89}/FRTG13, Gal80; UAS-mGFP/+. (F) Mid-pupal SOG neurons in *retn*-Gal4^{89}/+ show dense arborization (arrowhead) and projections extending towards the protocerebrum (arrows). (G) Mid-pupal SOG neurons in *retn*-Gal4^{89} homozygous clones have little dendritic branching (arrowhead) and poor extension of distal processes (arrows). G is at a higher magnification than F. (H) Confocal section of midline-crossing transect (F) shows tight fasciculation of neurites (arrow). (I) Confocal sections of SOG transect (G) shows poor fasciculation of the same neuronal projections (arrow). (J) Mid-pupal photoreceptors R1-R6 project to the lamina (LA), while faint pattern of R8 projections (arrow) is visible in the medulla (ME). (K) In *retn*-Gal4^{89} homozygous tissue, subsets of R1-R6 cells extend beyond the lamina into the medulla (arrow). A-I, anterior is upwards; J,K, anterior towards the left.

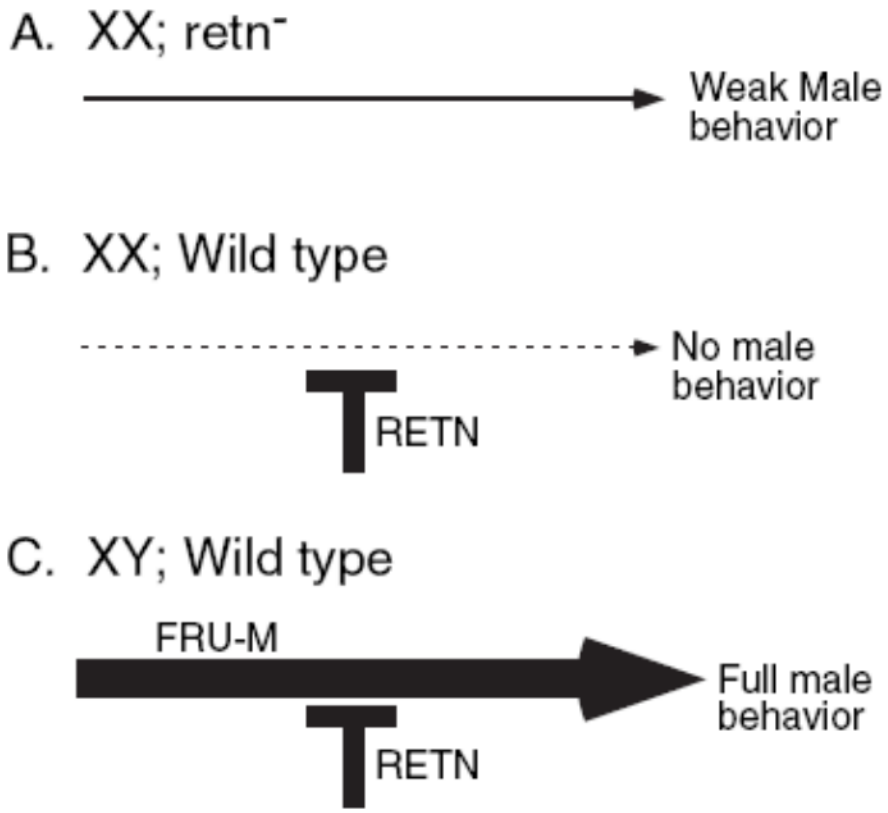

Fig 8. A model for the relationship between *retn* and *fru* functions in male behavior

(A) In the absence of *retn* or *fru* functions, there is an intrinsic tendency towards development of neural circuitry leading to male-like courtship. In situations in which *retn* and the *fru*M products are absent, such as in *retn* mutant females, this will be revealed as some degree of male-like courtship behavior. (B) The *retn* products normally act to counter the tendency towards male-like behaviors such that wild-type females do not show male-like behavior. (C) In wild-type males, *retn* is still active as a repressor, but the presence of *fru*M product substantially enhances development of the male behavior pathway, such that the male behavior pathway overcomes the negative effect of *retn* function.